ADVANCED MATERIALS

[5] D. W. Berreman, *Phys. Rev. Lett.* **1972**, *28*, 1683.
[6] M. F. Toney, T. P. Russell, J. A. Logan, H. Kikuchi, J. M. Sands, S. K. Kumar, *Nature* **1995**, *374*, 709.
[7] M. Schadt, K. Schmitt, V. Kozinkov, V. Chigrinov, *Jpn. J. Appl. Phys., Part 1* **1992**, *31*, 2155.
[8] W. M Gibbons, P. J. Shannon, S. T. Sun, B. J. Sweltin, *Nature* **1991**, *351*, 49.
[9] G. P. Bryan-Brown, C. V. Brown, I. C. Sage, V. C. Hui, *Nature* **1998**, *392*, 365.
[10] P. Chaudhari, J. Lacey, J. Doyle, E. Galligan, S. C. A. Lien, A. Callegari, G. Hougham, N. D. Lang, P. S. Andry, R. John, K. H. Yang, M. H. Lu, C. Cai, J. Speidell, S. Purushothaman, J. Ritsko, M. Samant, J. Stohr, Y. Nakagawa, Y. Katoh, Y. Saitoh, K. Sakai, H. Satoh, S. Odahara, H. Nakano, J. Nakagaki, Y. Shiota, *Nature* **2001**, *411*, 56.
[11] G. Maret, K. Dransfeld, in *Strong and Ultrastrong Magnetic Fields and Their Applications* (Ed: F. Herlach), Springer, New York **1985**, pp. 143–204.
[12] M. I. Boamfa, M. W. Kim, J. C. Maan, T. Rasing, *Nature* **2003**, *421*, 149.
[13] See for example: P. G. de Gennes, J. Prost, *The Physics of Liquid Crystals*, 2nd ed., Clarendon, Oxford, UK **1993**.
[14] M. I. Boamfa, *Ph.D. Thesis*, University of Nijmegen **2003**.
[15] M. B. Feller, W. Chen, Y. R. Shen, *Phys. Rev. A: At., Mol., Opt. Phys.* **1991**, *43*, 6778.
[16] G. Barbero, N. V. Madhusudana, J. F. Palierne, G. Durnad, *Phys. Lett. A* **1984**, *103*, 385.
[17] E. C. M. Vermolen, presented at the 10th Intl. Topical Mtg. on Optics of Liquid Crystals, Aussios, France, September 2003.

Spinning Solid and Hollow Polymer-Free Carbon Nanotube Fibers**

By *Mikhail E. Kozlov*,* *Ryan C. Capps*, *William M. Sampson*, *Von Howard Ebron*, *John P. Ferraris*, and *Ray H. Baughman**

A flocculation-based process has been developed for spinning polymer-free carbon nanotube fibers from aqueous dispersions. This spinning process works for single-walled nanotubes (SWNTs), double-walled nanotubes, one-to-three mixtures by weight of single- and multiwalled nanotubes, and one-to-one mixtures by weight of single-walled nanotubes and imogolite (a naturally occurring silicate nanofiber). It produces hollow fibers, folded ribbon fibers, and solid fibers, meaning those without aggregated space. After annealing, the fibers spun from the SWNTs exhibited relatively high electrical conductivities (~140 S cm^{-1} at room temperature) and high values of mass-normalized electrochemical capacitance (~100 F g^{-1}). Polarized Raman measurements indicate partial nanotube alignment in the spun fibers. Fiber supercapacitors were fabricated using these spun fibers.

Individual SWNTs have remarkable properties, including high strength, modulus, and electrical and thermal conductivities.[1] In order to utilize these properties for most applications, the individual nanotubes must be assembled into macroscopic structures like fibers, ribbons, and films. Spinning SWNT/poly(vinyl alcohol) (PVA) composite fibers was initially reported by Vigolo et al.[2] and further advanced by Dalton et al.[3] This process involves injection of surfactant-dispersed SWNTs into a flowing solution of aqueous PVA to produce gel fibers, which are optionally washed and then dried.

When PVA is largely retained, the obtainable SWNT/polymer composite fibers are quite strong, with toughness values over an order of magnitude higher than those previously reported for graphite fibers and synthetic organic fibers.[3] However, reflecting the high loading of PVA (over 40 wt.-%), which is a non-conductive polymer, the electrical and thermal conductivities of these nanotube/polymer composite fibers are much lower than can be obtained for SWNT sheets (bucky paper).[4] The presence of this polymer is problematic for applications such as fiber-based artificial muscles and supercapacitors, which require high electrochemical accessibility to the nanotubes and high electrical conductivity of the fibers.

In a process developed at Rice University,[5] SWNTs are first dispersed in 102 % sulfuric acid and then wet-spun into either diethyl ether, 5 % sulfuric acid, or water. Very high nanotube concentrations in the spinning solutions are possible for this superacid spinning and the achieved nanotube orientation and electrical and thermal conductivities are very high. However, some protonation of the material occurs because of prolonged contact with the sulfuric acid and, like for superacid processes used in industry, special protection equipment is needed.

The presently described wet-spinning process provides polymer-free nanotube fibers without the need for superacids. The fibers are spun from solutions comprising nanotubes, surfactant, and water. Various types of nanotubes have been spun by this method, including HiPco SWNTs obtained from a carbon-monoxide process (Carbon Nanotechnologies Inc.), SWNTs prepared by laser ablation (Carbon Nanotechnologies Inc.), double-walled nanotubes (Nanocyl Inc.), mixtures of HiPco SWNTs and multiwalled nanotubes (Sunnano Inc.), and mixtures of SWNTs and naturally occurring silicate nanofibers (imogolite). However, the focus of this paper is on fibers spun from HiPco SWNTs.

Like the polymer-based coagulant spinning method and unlike the superacid spinning, the polymer-free spinning process utilizes dilute, low-viscosity dispersions of carbon nanotubes (about 0.6 wt.-% or lower SWNT content). However, unlike either of these previous methods, neither the spinning solution nor the coagulation fluid is very viscous. The polymer-free method works because the stream of spinning solution is stable against breakup up to the point of coagulation and the flocculated fiber does not fragment in the flow field. In addi-

[*] Dr. M. E. Kozlov, Prof. R. H. Baughman, R. C. Capps, W. M. Sampson, Dr. V. H. Ebron, Prof. J. P. Ferraris
The NanoTech Institute
University of Texas at Dallas
Richardson, TX 75080 (USA)
E-mail: Mikhail.Kozlov@utdallas.edu; Ray.Baughman@utdallas.edu

[**] This work was supported by DARPA grant MDA 972-02-C-005, DOD/USARO grant W911NF-04-1-0174, the Texas Advanced Technology Program grant 009741-0130-2003, and the Robert A. Welch Foundation.

  DOI: 10.1002/adma.200401130

tion, hollow fibers can be spun using the present polymer-free flocculation method.

The strategy for the present polymer-free spinning is to use either acidic or basic flocculation solutions to disrupt the surfactant-stabilized nanotube dispersions. This disruption, to produce the gel fiber, must occur rapidly and uniformly, otherwise the injected stream of spinning solution breaks into unconnected segments of aggregated nanotubes. While it is well-known that changing the pH of a solution of dispersed nanoparticles can result in particle aggregation,[6] which is called either flocculation or coagulation, it is quite unusual that such aggregation can produce continuous fibers.

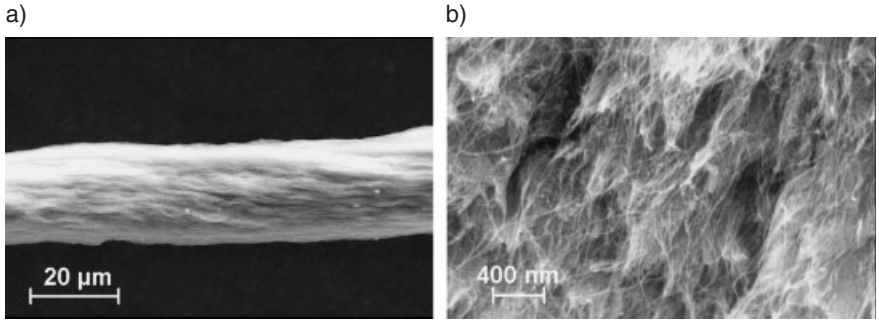

Figure 1. SEM images of fibers taken at low (left) and high (right) magnification. A degree of nanotube alignment is suggested by the sidewall structure (left image) and a low-density SWNT network (right image) is apparent.

We narrowed down a selection of acids and bases for the flocculation-based spinning process by observing flocculation as a function of adding various acids (hydrochloric, sulfuric, nitric, and phosphoric) or bases (NaOH and KOH) to surfactant-stabilized dispersions of carbon nanotubes in water. All of these acids and bases caused essentially instantaneous flocculation when the pH changed from almost neutral for the nanotube dispersion to strongly alkaline ($pH > 13$) or acidic ($pH < 1$). While any of the mentioned acids and bases could be used for nanotube spinning, we describe results obtained using 37 % HCl as the flocculation agent. The spinning solution used was essentially the same lithium-dodecyl-sulfate-stabilized (LDS-stabilized) aqueous dispersion employed for spinning supertough SWNT/PVA composite fibers.[3]

For the spinning experiments described here, 0.6 wt.-% HiPco SWNTs were dispersed using a horn sonicator in an aqueous solution of 1.2 wt.-% LDS surfactant. A narrow jet of this spinning solution was injected into the flocculation bath containing 37 % hydrochloric acid, which rotated at 33 rpm. The configuration of the rotating bath and spinneret needle was similar to that described for PVA-based coagulation spinning.[2] Flocculation of nanotubes in the spinning solution to form a gel fiber occurred very close to the point of contact of the spinning solution and the acid in the bath. This gel fiber (containing 90 wt.-% volatilizable liquid based on gravimetric measurements) was washed in methanol to remove the hydrochloric acid. The fiber, which had a very low elasticity both before and after the washing step, was then pulled from the wash bath, stretched over a frame, and dried under tension. In some experiments, this dried fiber was annealed at 1000 °C in argon for an hour in order to remove possible residual impurities.

Scanning electron microscopy (SEM) images of the dried fibers are shown in Figure 1. The spun fibers typically had diameters of 10–50 μm. The structure of their lateral surfaces suggests a degree of nanotube alignment (Fig. 1, left panel) and fiber-fracture surfaces show a well-resolved network of SWNT bundles (Fig. 1, right panel).

The Raman spectra (632.8 nm excitation wavelength) of the fibers spun using the various flocculating agents closely resembled the Raman spectrum of the pristine nanotubes. However, the intensity of the Raman lines changed when polarized light was used. This was due to the well-known fact that the Raman intensity in VV configuration (excitation and detection in the same polarization plane) for the tangential mode (G-line) decreases continuously as the angle between the nanotube axis and the direction of polarization increases.[7] The ratio of the Raman intensity for light parallel and perpendicular to the fiber axis was ~5, indicating that the nanotubes were partially oriented parallel to the fiber axis, in agreement with our SEM observations.

Novel hollow fibers (Figs. 2A,B), which are quite unlike the solid fibers reported to date for PVA-based and superacid-based nanotube spinning, could be obtained by using an injection rate of about 0.70 mL min^{-1} and an inner spinneret diameter of 500 μm. Under similar spinning conditions, fibers with the appearance of a partially collapsed ribbon fiber could also result (Fig. 2C). Solid fibers with a diameter of about 15 μm or less could be obtained by using a lower injection rate (~0.25 mL min^{-1}), and these narrow fibers appeared to result from the complete collapse of the gel ribbon fiber. Like in PVA-based spinning, the cylindrical stream of spinning solution collapsed into this gel ribbon. However, unlike the case of PVA-based spinning, this gel ribbon was stable against collapse into a solid fiber (unless the lateral dimensions of the gel fiber were small). So in all, the gel ribbon could scroll to form hollow fibers (Figs. 2A,B), could fold to form the cross-section shown in Figure 2C, or could fully collapse to form the "solid" cross-section of Figure 2D. These hollow (cylinder-like and continuous along the circumference) and folded-ribbon structures are interesting for possible applications in which it is desirable to decrease diffusion distances between species in a surrounding liquid and the mass of the nanotube fiber, such as in nanotube electrochemical devices (fiber supercapacitors, batteries, and artificial muscles) and in nanotube-fiber-based filtration and absorption (including absorption-based sensors). However, such non-compact geometries are undesirable when the goal is to

ADVANCED MATERIALS

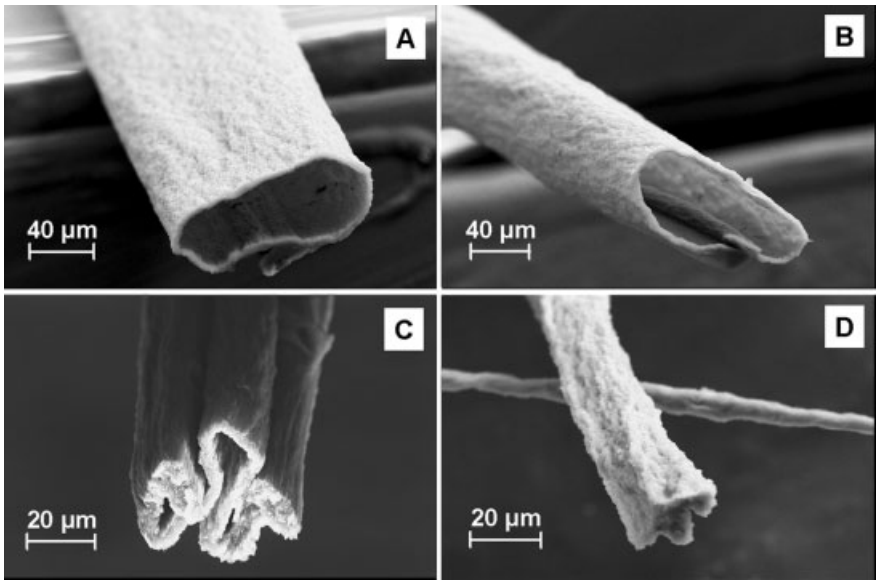

Figure 2. Cross-sections of different as-spun fibers: hollow (A, B), folded ribbon (C), and solid (D).

optimize absolute mechanical properties, rather than mechanical properties normalized to fiber density.

Thermogravimetric analysis (TGA) data in Figure 3 shows that the spun HiPco nanotubes were more stable with respect to combustion in oxygen gas than the pristine nanotubes from which they were spun. The substantial residual-weight fraction after combustion for both samples is due to the iron catalyst in the HiPco nanotubes,[8] which apparently did not interfere with the spinning process since the corresponding volume fraction of iron or iron oxide was low (a few volume percent). The initial weight increase during combustion (due to oxidation of the iron catalyst) and the residual weight after combustion were both smaller for the nanotube fiber than for the as-synthesized HiPco nanotubes, indicating that the content of iron catalyst decreased during spinning. This fact is consistent with the data for HiPco treated with HCl, an acid widely used in the nanotube-purification process.[8] The increased stability of the spun fibers with respect to combustion is likely to be a result of this decrease in iron content (which catalyzes combustion) and the higher packing density of nanotubes in the fiber than in the as-synthesized nanotubes.

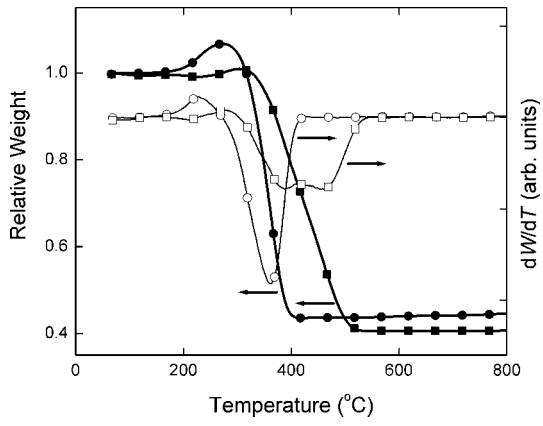

Figure 3. Fraction of retained weight versus temperature during the heating of pristine HiPco nanotubes (●) and HiPco fibers (■) in flowing oxygen at 5 °C min^{-1}. The derivatives, dW/dT, of these weight-loss curves for the pristine nanotubes (○) and the spun fibers (□) are also shown.

The mechanical properties were determined directly, on a density-normalized basis, from force measurements, the fiber length, and the fiber weight per fiber length. This approach was used to eliminate uncertainties in the fiber cross-section that could be quite large, especially when the cross-section was irregular. Such density-normalized mechanical properties are especially relevant when the weight of the structural element is important, such as in aerospace applications. This approach provides a lower bound on the tensile strength at the location of fiber failure. These measurements resulted in a density-normalized specific stress of 65 MPa g^{-1} cm^{-3}, Young's modulus of 12 GPa g^{-1} cm^{-3}, and a strain-to-failure of about 1 %. These mechanical properties reflect the low degree of mechanical coupling achieved between individual nanotube bundles. To improve this coupling, we infiltrated PVA in the as-spun gel fibers (before washing in methanol) by soaking these fibers in a 5 % aqueous solution of this polymer, and drying. The mechanical properties dramatically increased to a maximum-achieved true tensile strength of 770 MPa g^{-1} cm^{-3}, a Young's modulus of 8.9 GPa g^{-1} cm^{-3}, a strain-to-failure of 30 %, and a fiber toughness of 137 J g^{-1}. While these values of strength and toughness are lower than the record values achieved for nanotube fibers spun using the PVA-coagulant process,[3] the toughness exceeds that of commercial fibers used for antiballistic protection and is close to the maximum toughness observed for spider silk.

Electrical-conductivity values were measured at room temperature using the four-probe method. The electrical conductivity, derived using the external cross-sectional area of the fiber measured by optical microscopy, increased from 15 S cm^{-1} for the as-spun fiber to 140 S cm^{-1} for the annealed fibers. While infiltration with PVA post-spinning dramatically improved the mechanical properties, this additional processing dramatically decreased the electrical conductivity to a value far below that of the as-spun fibers.

The specific capacitance of the polymer-free fibers was measured using a three-electrode cell with carbon felt as the counter electrode, Ag/Ag$^+$ as the reference electrode, and the ionic liquid, ethylmethylimidazolium trifluoromethylsulfonyl imide, as the electrolyte. The measured fiber capaci-

tances for the as-spun and annealed fibers were 48 and 100 $F\,g^{-1}$, respectively, which are substantially higher than the 10 to 30 $F\,g^{-1}$ that we typically obtain for nanotube sheets. These fibers were used to fabricate fiber supercapacitors by coating the fibers separately with a polymer ionic liquid–solid electrolyte system (methyl methacrylate polymerized in the presence of the ionic liquid electrolyte, ethylmethylimidazolium trifluoromethylsulfonyl imide), combining the coated fibers, and recoating with the same electrolyte. The fiber supercapacitors gave a specific capacitance of 7 $F\,g^{-1}$ (based on total device weight) when cycled in the ±1.5 V potential window at 5 $mV\,s^{-1}$. Charge–discharge studies are currently being performed to further characterize device performance and will be reported separately.

The polymer-free fibers prepared using the present process provide substantially increased electrical conductivity compared with nanotube-composite fibers with high polymer loadings obtained using polymer-based coagulation spinning (0.2 $S\,cm^{-1}$ or lower for SWNT/PVA fibers comprising 60 % SWNTs). In addition, they provide the very high capacitance needed for application as supercapacitors and artificial muscles. The results presented show that post-spinning addition of polymer can dramatically increase the mechanical properties by indirectly mechanically coupling nanotubes, but the electrical conductivity is dramatically decreased. The achieved hollow-fiber structures are unprecedented for directly spun polymer-free fibers, and suggest applications such as materials separation, materials absorption, and sensing.

Experimental

The SWNT/PVA composite fibers utilized a 5 % solution of PVA (J. T. Baker Chemicals, M_W: 77 000–79 000, 99.0–99.8 % hydrolyzed). The gel fibers were immersed in this polymer solution immediately after spinning and soaked for 24 h prior to drying in ambient conditions.

SEM images were acquired using a LEO 1530 field-emission scanning electron microscope. Raman spectroscopy measurements were performed using a Jobin Yvon LabRam HR800 Raman Microscope equipped with a He:Ne laser ($\lambda = 632.8$ nm). Mechanical properties were characterized using an Instron 5848 Micro Tester. Electrical conductivity measurements were carried out using the conventional four-probe method at room temperature. Thermogravimetric data for the material were collected using a Perkin Elmer Thermogravimetric Analyzer Pyris1 TGA. The measurements were carried out from room temperature to 1000 °C at a heating rate of 5 °C min^{-1} in flowing oxygen.

Cyclic voltammetry experiments were performed using a Princeton Applied Research EG&G 273A Potentiostat/Galvanostat.

Received: July 14, 2004
Final version: November 18, 2004

[1] R. H. Baughman, A. A. Zakhidov, W. A. de Heer, *Science* **2002**, *297*, 787.

[2] a) B. Vigolo, A. Pénicaud, C. Coulon, C. Sauder, R. Pailler, C. Journet, P. Bernier, P. Poulin, *Science* **2000**, *290*, 1331. b) B. Vigolo, P. Poulin, M. Lucas, P. Launois, P. Bernier, *Appl. Phys. Lett.* **2002**, *81*, 1210.

[3] A. B. Dalton, S. Collins, E. Munoz, J. Razal, V. H. Ebron, J. P. Ferraris, J. N. Coleman, B. G. Kim, R. H. Baughman, *Nature* **2003**, *423*, 703.

[4] A. G. Rinzler, J. Liu, H. Dai, P. Nikolaev, C. B. Huffman, F. J. Rodriguez-Macias, P. J. Boul, A. H. Lu, D. Heymann, D. T. Colbert, R. S. Lee, J. E. Fischer, A. M. Rao, P. C. Eklund, R. E. Smalley, *Appl. Phys. A* **1998**, *67*, 29.

[5] a) V. A. Davis, L. M. Ericson, A. N. G. Parra-Vasquez, H. Fan, Y. Wang, V. Prieto, J. A. Longoria, S. Ramesh, R. K. Saini, C. Kittrell, W. E. Billups, W. W. Adams, R. H. Hauge, R. E. Smalley, M. Pasquali, *Macromolecules* **2004**, *37*, 154. b) W. Zhou, J. Vavro, C. Guthy, K. I. Winey, J. E. Fischer, L. M. Ericson, S. Ramesh, R. Saini, V. A. Davis, C. Kittrell, M. Pasquali, R. H. Hauge, R. E. Smalley, *J. Appl. Phys.* **2004**, *95*, 649. c) L. M. Ericson, H. Fan, H. Peng, V. A. Davis, W. Zhou, J. Sulpizio, Y. Wang, R. Booker, J. Vavro, C. Guthy, A. N. G. Parra-Vasquez, M. J. Kim, S. Ramesh, R. Saini, C. Kittrell, G. Lavin, H. Schmidt, W. W. Adams, W. E. Billups, M. Pasquali, W.-F. Hwang, R. H. Hauge, J. E. Fischer, R. E. Smalley, *Science* **2004**, *305*, 1447.

[6] K. Holmberg, B. Jönsson, B. Kronberg, B. Lindman, *Surfactants and Polymers in Aqueous Solution*, 2nd ed., John Wiley & Sons, New York **2002**.

[7] A. Jorio, A. G. Souza Filho, V. W. Brar, A. K. Swan, M. S. Unlu, B. B. Goldberg, A. Righi, J. H. Hafner, C. M. Lieber, R. Saito, G. Dresselhaus, M. S. Dresselhaus, *Phys. Rev. B* **2002**, *65*, 121 402(R).

[8] W. Zhou, Y. H. Ooi, R. Russo, P. Papanek, D. E. Luzzi, J. E. Fischer, M. J. Bronikowski, P. A. Willis, R. E. Smalley, *Chem. Phys. Lett.* **2001**, *350*, 6.

Controlled Assembly of Protein–Nanoparticle Composites through Protein Surface Recognition**

By *Sudhanshu Srivastava*, *Ayush Verma*, *Benjamin L. Frankamp*, and *Vincent M. Rotello**

Protein-mediated assembly of nanoparticles is a potent tool for the creation of new materials.[1,2] These materials combine tunable nanoparticle features (size, surface functionality, and core properties)[3] with the unique physical and chemical properties of proteins[4] and peptides.[5] Recently, the use of nanoparticles has enabled fabrication of protein–nanoparticle conjugates using tailored protein units as linkers.[6–8] To date, however, this approach has been limited to the synthetic modification of the nanoparticle to directly interact with anti-

[*] Prof. V. M. Rotello, S. Srivastava, A. Verma, B. L. Frankamp
Department of Chemistry, University of Massachusetts at Amherst
Amherst, MA 01003 (USA)
E-mail: rotello@chem.umass.edu

[**] This research was supported by the National Institutes of Health (NIH, GM 62998) and the National Science Foundation (NSF, CHE-0213354, and MRSEC facilities). We acknowledge Nicholas O. Fischer for figure preparations. B. L. F. acknowledges the ACS Division of Organic Chemistry Graduate Fellowship sponsored by the Proctor and Gamble Company. Supporting Information is available online from Wiley InterScience or from the author.

 DOI: 10.1002/adma.200400776